

# Numerical Investigation of heat penetration on cutting force during laser assisted machining of Ti6Al4V

Muruga Prabu U#, Afzaal Ahmed and Pramod Kuntikana

Department of Mechanical Engineering, Indian Institute of Technology, Ahalia Integrated Campus, Kozhippara, Kerala 678557  
# Corresponding Author / Email: 132114005@smail.iitpkd.ac.in, TEL: +91-9486151020

KEYWORDS: Laser assisted machining, Cutting force, Ti6Al4V

*The applications of superalloys like Ti6Al4V have rapidly increased over the years in aerospace, biomedical and chemical industries. This is attributed to the exceptional physical and mechanical properties like high melting point, retention of properties at elevated temperatures and high toughness. Nevertheless, these properties pose challenges in processing Ti6Al4V by conventional machining methods. Laser assisted machining (LAM) is one of the hybrid machining processes which is employed to overcome these challenges. During LAM, the phenomenon of material softening at elevated temperatures results in reduction of the cutting force which consequently leads to lower specific energy consumption. Owing to the dynamic and non-linear nature of the machining processes, the numerical simulation of these processes becomes complex. In case of laser assisted machining, the complexity of the simulation increases further because of the interdependence of the laser parameters and the mechanism of material removal. A numerical model is proposed in this study to predict the cutting force at different feed rates keeping the laser heat flux and cutting speed constant. The thermal softening effect is modeled using the Johnson-Cook material constitutive equations. A significant reduction in cutting force was observed due to laser assistance and the penetration depth condition with respect to uncut chip thickness for minimum cutting force has been identified and elaborated.*

## NOMENCLATURE

$F_c$  = Cutting force (N)  
 $h$  = uncut chip thickness (mm)  
 $d$  = laser penetration depth (mm)

## 1. Introduction

With the increased use of superalloys such as Inconel 718 and Ti-6Al-4V in the oil and gas, aerospace, automotive, and biomedical industries, machining these superalloys with conventional methods has become more difficult. When conventional machining methods are employed to cut such materials, rapid tool wear and loss of productivity were predominant. Other disadvantages of conventional superalloy machining include high cutting forces and poor surface finish.

To address these shortcomings, researchers used heat assistance to ease the machining process by lowering the workpiece's strength

and hardness prior to machining. Heat sources such as gas flames, induction coils, plasma, and lasers were employed to machine such difficult-to-cut superalloys. Lasers have been the most popular of these heat sources due to their high energy density and ease of control.

### 1.1. Literature review on experimental work in LAM

The first few studies on LAM were conducted in the 1980s. Rajagopal et al. [1] conducted studies on the benefits of LAM on aerospace alloys. The authors showed a 100 % gain in MRR during LAM on Ti6Al4V without significant increase in cutting force. An economic analysis of the LAM process on Inconel 718 established that it was 66% less expensive than conventional carbide machining [2]. In another study, a hybrid LAM process combining LAM and cryogenic tool cooling was demonstrated [3]. A two-fold increase in tool life during the hybrid machining was revealed by the authors. The process parameters were optimized in a couple of studies conducted by Rashid et al. [11, 12]

### 1.2. Literature review on numerical study in LAM

Due to the interdependence of heating and machining mechanisms, simulation of laser assisted machining is a complex process. Shi et al. [4] and Pan et al. [5] used DEFORM 3D software to run LAM simulations. The authors proved the occurrence of thermal softening effect during LAM using simulations. Abaqus/Explicit solver was employed by Germain et al. [6] and Venkatesan et al. [7] to execute LAM simulations. The authors investigated the effect of laser power, feed rate, and cutting speed on cutting force. Ayed et al. [8] investigated the relationship between cutting force and the distance between the laser beam and the tool rake face. However, the effect of laser penetration depth(d) on the LAM process has yet to be investigated. The effect of laser penetration depth on cutting force and uncut chip temperature is investigated in the present work and the optimal laser penetration depth condition is identified and has been elaborated.

## 2. Simulation of laser assisted machining process

### 2.1 Methodology

Figure 1 depicts a schematic representation of the laser assisted machining (LAM) process. Thermal and machining simulations are both included in the 2D LAM numerical study. The temperature output of the thermal simulation is fed as an input to the machining simulation.

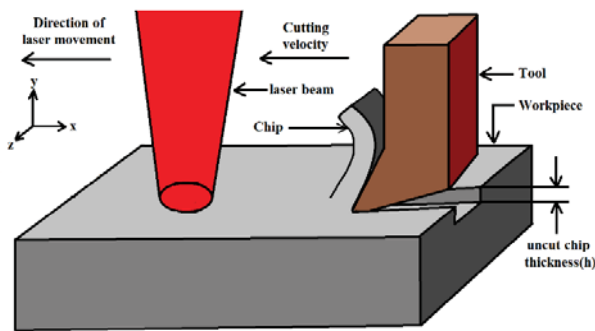


Fig. 1 Schematic of the laser assisted machining process

Fig. 2 displays the flow diagram outlining the methodology employed for simulations. For the numerical investigation, Abaqus/Explicit (version 2020) software was used. Abaqus was used due to its mesh distortion control feature which outperforms the remeshing methods of other commercial packages.

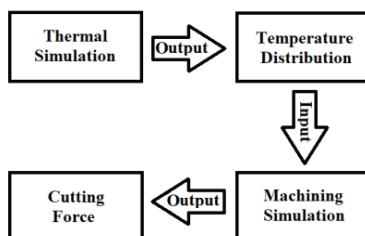


Fig. 2. Block diagram explaining the simulation flow

Ti6Al4V workpiece of dimension 3 mm × 1.2 mm is geometrically modeled for the study. The rake angle and clearance angle of the tungsten carbide tool are 17.5 ° and 7 ° respectively. Table 1 shows the properties of the tool and workpiece.

Table 1 Properties of the workpiece and tool

Physical parameters	Workpiece (Ti6Al4V)	Tool (Tungsten carbide)
Elastic modulus E (GPa)	110	705
Poisson's ratio $\nu$	0.33	0.23
Density $\rho$ (kg/m <sup>3</sup> )	4430	15700
Thermal conductivity $\lambda$ (W/m °C)	6.6	24
Specific heat $C_p$ (J/kg °C)	670	178

The other parameter settings for the study are laser speed - 40 m/min, laser flux - 300 W/mm<sup>2</sup> and laser spot size - 0.8 mm. A 20  $\mu$ m thin sacrificial layer is utilized for the purpose of simulating the material separation that occurs during chip production. A four-node bilinear displacement and temperature, reduced integration with hourglass control (CPE4RT) elements with a minimum 10  $\mu$ m size are used to discretize the workpiece and tool domain. The workpiece-tool interaction is handled by the penalty contact algorithm. Insulated thermal boundary condition is assumed for the tool and workpiece. The workpiece and the tool initial temperature are 25° C. Johnson-Cook material constitutive equations are used to model the thermal softening effect. Table 2 shows the simulation parameters.

Table 2 Simulation details and conditions

Details	Conditions
Geometry	2D (plain strain)
Workpiece	Ti6Al4V
Tool	Tungsten carbide
Solution method	Coupled Temperature-Displacement Explicit
Mesh type	CPE4RT
Contact Algorithm	Penalty
No. of elements in workpiece	9570
No. of elements in tool	882

#### 2.1.1 Johnson-Cook(J-C) material constitutive model

The J-C plasticity model is often used to describe the relationship between material stress and strain under different conditions of strain rates and temperatures. The equation describing the model is given below.

$$\sigma = (A + B\varepsilon^n)(1 + C_1 \ln \dot{\varepsilon}^*)(1 - T^{*m}) \quad (1)$$

where  $\sigma$  is the von Mises equivalent yield stress,  $\epsilon$  is the equivalent plastic strain,  $\dot{\epsilon}^*$  is the dimensionless strain rate,  $T^*$  is the dimensionless temperature,  $A$  is the yield stress at a reference strain rate and reference temperature,  $B$  is the material hardening coefficient,  $n$  is the material strain hardening exponent,  $C_1$  is the strain rate sensitivity factor, and  $m$  is the temperature softening exponent. Material damage is modelled using the J-C damage equation given below.

$$\epsilon^f = (D_1 + D_2 e^{D_3 \sigma^*})(1 + D_4 \ln(\dot{\epsilon}^*))(1 + D_5 T^*) \quad (2)$$

where  $\epsilon^f$  is the equivalent strain at failure,  $D_1 - D_5$  are the J-C failure parameters. J-C parameters of Ti6Al4V are shown in table 3.

Table 3 J-C plasticity and damage parameters [9,10]

Parameter	Value
A (MPa)	783
B (MPa)	498
n	0.28
C	0.028
m	1.0
$D_1$	-0.09
$D_2$	0.25
$D_3$	-0.5
$D_4$	0.014
$D_5$	3.87

### 3. Results and Discussion

The results are analyzed based on the relationship between the laser penetration depth( $d$ ) and uncut chip thickness( $h$ ). Three cases have been identified as depicted in table 2. In order to meet these cases the values of  $h$  are considered to be 0.3 mm, 0.2 mm, and 0.1 mm respectively and simulations were carried out at those precise values both with and without laser aid.

Table 2 The different cases of laser penetration depth considered for simulation

Case	1	2	3
Condition	$d < h$	$d = h$	$d > h$

$d$  = heat penetration depth;  $h$  = uncut chip thickness

#### 3.1. Effect of penetration depth on uncut chip temperature

In Fig. 3, the thermal simulation is shown indicating the laser spot and penetration depth. From the temperature contour, the height from the surface of the workpiece till the depth up to which the temperature change occurs is defined as the penetration depth ( $d$ ). The laser penetration depth which is a function of material thermal diffusivity and time of exposure is measured to be 0.2 mm for Ti6Al4V at a laser speed and flux of 40 m/min and 300 W/mm<sup>2</sup> respectively. Using the 'history output' option of Abaqus, the temperature of all the nodes

present in the uncut chip region is obtained and the average temperature ( $T_{ave}$ ) is computed. From Fig. 4, it is found that  $T_{ave}$  rises as the laser penetration depth increases with respect to uncut chip thickness. The minimum value of  $T_{ave}$  was 352 °C when  $d < h$ .  $T_{ave}$  reaches a maximum value of 760 °C for the condition  $d > h$ . Subsequently, these temperature values from the thermal study are fed as input to the machining simulations.

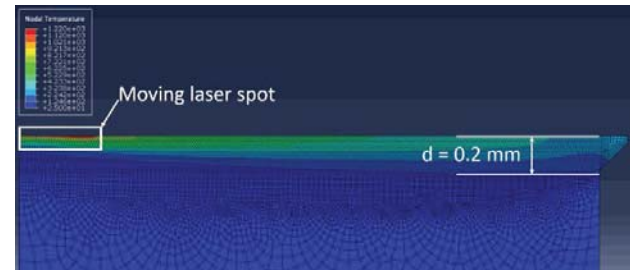


Fig. 3. Thermal simulation result showing the temperature distribution

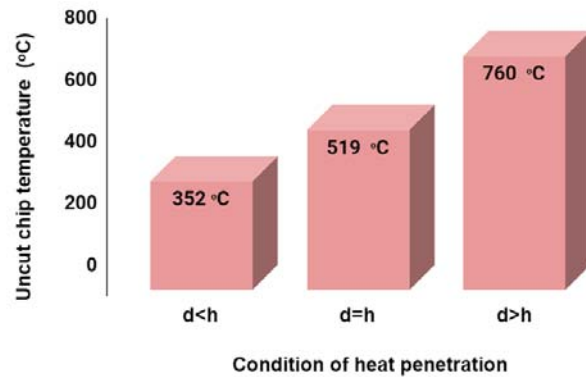


Fig. 4. Uncut chip temperature for the different scenarios

#### 3.2. Effect of penetration depth on cutting force

Fig. 5 shows cutting force distribution at a particular instant of time ( $t=2.58e^{-03}$  s) from the machining simulations. From Fig. 5, the magnitude of instantaneous maximum cutting force was found to be 45 N for the case  $d < h$  and the instantaneous minimum cutting force of 19 N occurs for the case  $d > h$ . Using the 'history output' option of Abaqus, the cutting force values are obtained at left face nodes of the workpiece. The sum of all these nodal cutting force values gives the total cutting force. In order to calculate the percentage reduction in cutting force, the machining simulations are carried out with and without laser heating. Consequently, the percentage reduction in cutting force due to the laser heat is calculated and plotted in Fig. 6. The plot shows that the percentage reduction in cutting force increases as the penetration depth increases. In the first case ( $d < h$ ), the reduction in cutting force is minimum at 13.21 %. In contrast, a maximum of 22.52 % cutting force reduction happens for the third case ( $d > h$ ). The reason for this trend is understood from the results shown in Fig. 4. From Fig. 4, the increase in penetration depth led to increase in uncut chip temperature. According to Johnson-Cook model, increase in temperature results in reduction of material yield

stress. Consequently, the cutting force decreases at a higher penetration depth. The findings were compared with experiments reported in the literature [8]. Cutting force range of 250-350 N observed from the experiments matched closely with the simulation results.

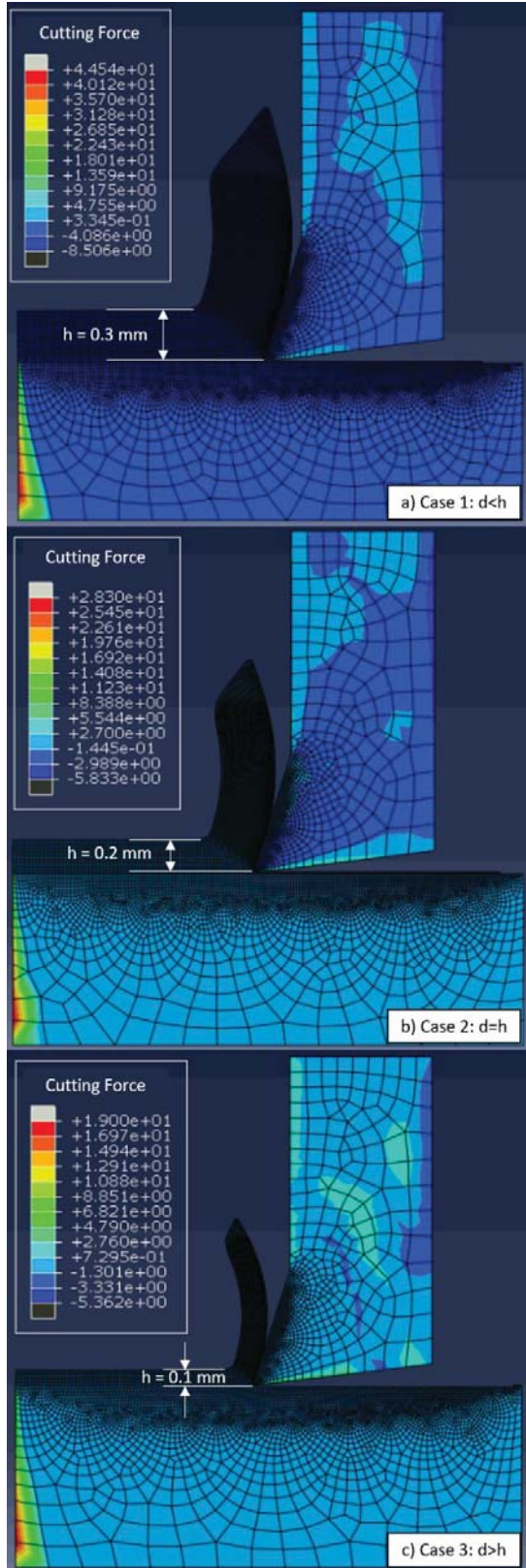


Fig. 5. Reaction force contour for the three cases.

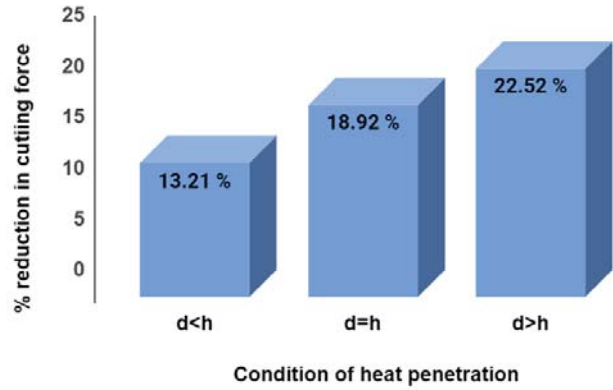


Fig. 6. Cutting force reduction vs laser penetration depth

### 3. Conclusions

The current numerical study analyzed the influence of laser penetration depth on the cutting force during machining of Ti6Al4V superalloy. Three cases of different uncut chip thickness values for a constant penetration depth are considered. When the laser penetration depth ( $d$ ) was more than the uncut chip thickness ( $d > h$ ), a maximum cutting force reduction of 22.52 % was attained. Therefore, the current study has demonstrated that the laser penetration depth should always be more than the uncut chip thickness in order to reduce the cutting force. Moreover, a maximum uncut chip temperature of 760 °C appear at the same  $d > h$  case proving the material softening happening at higher temperatures. The findings of this work will undoubtedly advance research into novel ways to numerically study and explain the LAM process. The current work, however, considers sequential modelling, in which a thermal simulation and a machining simulation are conducted in successive steps. Additionally, future work will concentrate on a simultaneous thermal and machining simulation which will be closer to the actual LAM process.

### ACKNOWLEDGEMENT

The authors are grateful to the Department of Mechanical Engineering and the Central Facility for Materials and Manufacturing (CFMM), Indian Institute of Technology Palakkad for providing the necessary software facilities for the work.

### REFERENCES

1. Rajagopal, S., Plankenhorn, D. J., & Hill, V. L. (1982). Machining aerospace alloys with the aid of a 15 kW laser. Journal of Applied Metalworking, 2(3), 170–184.

2. Anderson, M., Patwa, R., & Shin, Y. C. (2006). Laser-assisted machining of Inconel 718 with an economic analysis. *International Journal of Machine Tools and Manufacture*, 46(14), 1879–1891.
3. Dandekar, C. R., Shin, Y. C., & Barnes, J. (2010). Machinability improvement of titanium alloy (Ti-6Al-4V) via LAM and hybrid machining. *International Journal of Machine Tools and Manufacture*, 50(2), 174–182.
4. Shi, B., Attia, H., Vargas, R., & Tavakoli, S. (2008). Numerical and experimental investigation of laser-assisted machining of inconel 718. *Machining Science and Technology*, 12(4), 498–513.
5. Pan, Z., Feng, Y., Lu, Y. T., Lin, Y. F., Hung, T. P., Hsu, F. C., Lin, C. F., Lu, Y. C., & Liang, S. Y. (2017). Microstructure-sensitive flow stress modeling for force prediction in laser assisted milling of Inconel 718. *Manufacturing Review*, 4.
6. Germain, G., Dal Santo, P., & Lebrun, J. L. (2011). Comprehension of chip formation in laser assisted machining. *International Journal of Machine Tools and Manufacture*, 51(3), 230–238.
7. Venkatesan, K., Kanubhai, J., Raval, G. V., & Vipulkumar, S. H. (2018). A Study on Prediction of Forces and Cutting Temperature in Laser-Assisted Machining of Inconel 718 Alloy Using Numerical Approach. *Materials Today: Proceedings*, 5(5), 12339–12348.
8. Ayed, Y., Germain, G., Salem, W. Ben, & Hamdi, H. (2014). Experimental and numerical study of laser-assisted machining of Ti6Al4V titanium alloy. *Finite Elements in Analysis and Design*, 92, 72–79.
9. W.-S. Lee, C.-F. Lin, High-temperature deformation behaviour of ti6al4v alloy evaluated by high strain-rate compression tests, *J. Mater. Process. Technol.* 75 (1–3) (1998) 127–136.
10. D. Lesuer, Experimental investigations of material models for Ti-6Al-4 V Titanium and 2024-T3 Aluminum. Final Report, DOT/FAA/AR-00/25, US Department of Transportation, Federal Aviation Administration; 2000.
11. Rahman Rashid, R. A., Sun, S., Wang, G., & Dargusch, M. S. (2012). The effect of laser power on the machinability of the Ti-6Cr-5Mo-5V-4Al beta titanium alloy during laser assisted machining. *International Journal of Machine Tools and Manufacture*, 63, 41–43.
12. Rahman Rashid, R. A., Sun, S., Wang, G., & Dargusch, M. S. (2012). An investigation of cutting forces and cutting temperatures during laser-assisted machining of the Ti-6Cr-5Mo-5V-4Al beta titanium alloy. *International Journal of Machine Tools and Manufacture*, 63, 58–69.